

Implementing Some Mathematical Models of Spiking Neurons

Zainab Alaa Abdulrazzaq¹

Thi-Qar University /Engineering College / Biomedical Engineering E-Mail: zanaibalaa1997@gmail.com

Basam wahad meteab²

Thi-Qar University /Engineering College / Biomedical Engineering E-Mail: powermoon908@gmail.com

Dhay Kadhim abbas³

Israa University / Medical Device Engineering College .Email: dhaykadhim99@gamil.com

Abstract

In this project we take various spiking neuron models, which are used in simulation or implementation of different spiking neural network applications; such as brain simulation and engineering problems. Biologically plausible and computational efficiency are the most important factors that will be taken in consideration in order to choose one from the available spiking neuron models. we have Hodgkin-Huxley Model (HH) is a mathematical model that describes how action potentials in neurons are initiated and propagated. It is a set of nonlinear differential equations it's normally Biologically plausible then we take three simple models of neurons in rodent brains (RTM, WB and Erisir models). These are similar models to Hodgkin-Huxley Model (HH) but with different parameter values finally Izhikevich Model is biologically plausible. As well as it is computationally efficient, as Izhikevich Model represented by two differential equations .The chosen model should be the best to fit and meet the application specifications. we are discussed these spiking neuron models mathematically and how it could be used in simulating hippocampus. As well as, this project considers valuable comparisons between these models which they are provided according to the biological plausibility, computational efficiency, number of variables and complexity.

Keywords: Spiking neuron models, Spiking neural network applications, Brain simulation, Engineering problems, Biologically plausible

Introduction

1.1 What Are Neurons?

Neurons are cells within the nervous system that communicate with each other by transmitting and receiving electrochemical signals called action potentials [1].

1.2 What Are the function of Neurons?

The main function of neurons is to receive, conduct, and transmit signals. Neurons carry signals from the sense organs inward to the central nervous system (CNS), which consists of the brain and spinal cord. In the CNS the signals are analyzed and interpreted by a system of neurons, which then produce a response. The response is sent, again by neurons, outward for action to muscle cells and glands [1].

1.3 What Are the Components of the Neuron?

A typical neuron consists of four parts:

1. Cell body or soma, containing the nucleus and other organelles.
2. Branches of dendrites, which receive signals from other neurons.
3. An axon which conducts signals away from the cell body.
4. Nerve terminals or presynaptic terminals are branches at the far end of the axon.

Nerve cells, body and axon, are surrounded by glial cells. These provide support for nerve cells and they also provide insulation sheaths called myelin that cover and protect most of the large axons. The combined number of neurons and glial cells in the human body is estimated at 10^{12} [1].

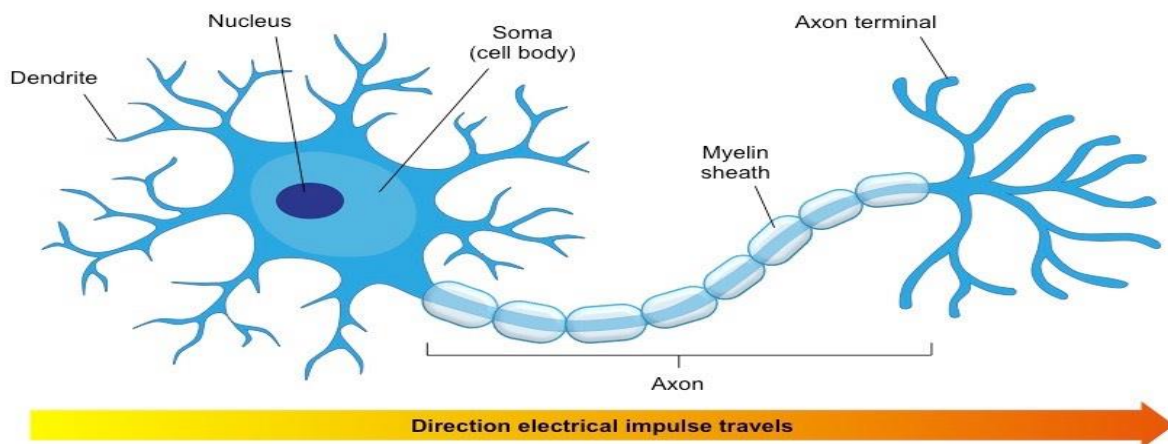


Figure 1.1 The structure of the neuron [*Quasar Jarosz CC BY SA 3.0, via Wikimedia Commons*]

1.4 How Neurons Work

The dendrites receive signals from nerve terminals of other neurons. These signals, tiny electric pulses, arrive at a location in the soma, called the axon hillock. The combined electrical stimulus at the hillock, if exceeding a certain threshold, triggers the initiation of a traveling wave of electrical excitation in the plasma membrane known as the action potential or voltage spike [1].

1.5 Action Potential.

Action potential is neuron communicate over long distances by generating and sending an electrical signal called a nerve impulse, or action potential [2].

1. To understand that rapid changes in permeability of the neuronal membrane produce the action potential.
2. To recognize that altering voltage-gated ion channels changes membrane permeability.
3. To understand the movement of sodium and potassium ions during the action potential.
4. To examine refractory periods.
5. To learn about conduction velocity.

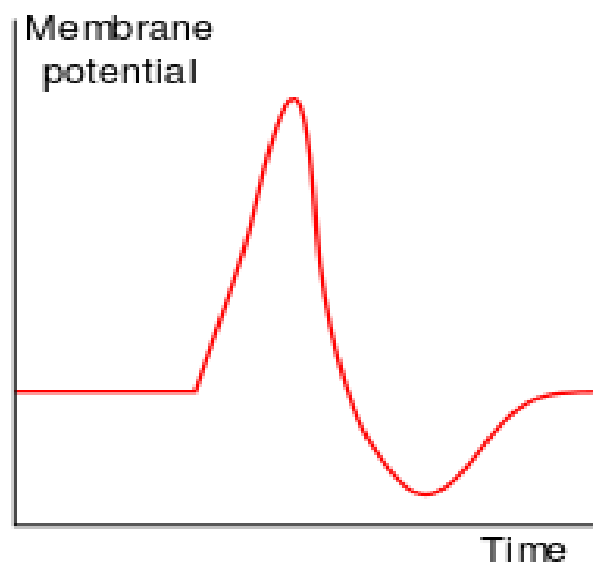


Figure 1.2 Shape of a typical Action Potential [*CC BY-SA 3.0*]

1.5.1 An Overview

1. The action potential is a large change in membrane potential from a resting value of about -70 millivolts to a peak of about +30 millivolts, and back to -70 millivolts again.

- The action potential results from a rapid change in the permeability of the neuronal membrane to sodium and potassium. The permeability changes as voltage-gated ion channels open and close.
- In the following pages we will study step-by-step the changes that occur as an action potential is generated and then propagated down the axon [3].

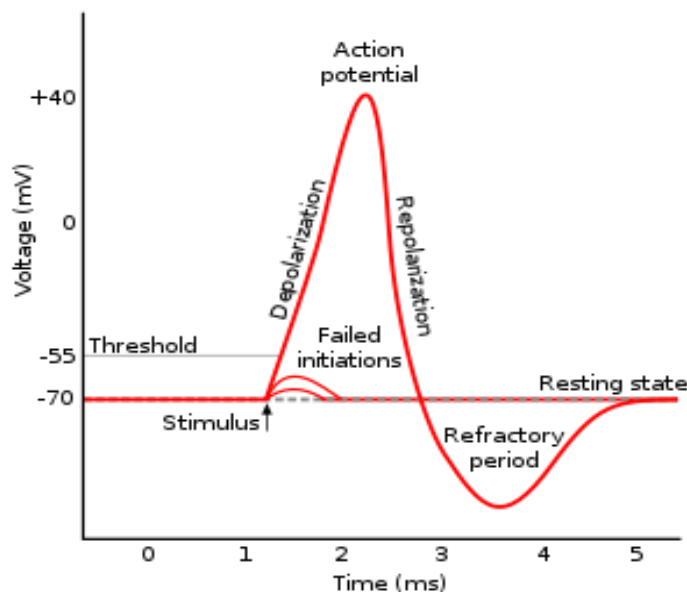


Figure 1.3 Process of Action Potential [*en:Image:ActionPotential.png*.]

1.5.2 The Action Potential Begins at the Axon Hillock

The action potential is generated at the axon hillock, where the density of voltage-gated sodium channels is greatest. The action potential begins when signals from the dendrites and cell body reach the axon hillock and cause the membrane potential there to become more positive, a process called depolarization. These local signals travel for only a short distance and are very different from action potentials [4],[5]. During Depolarization Sodium moves into the Neuron. As the axon hillock depolarizes, voltage-gated channels for sodium open rapidly, increasing membrane permeability to sodium. Sodium moves down its electrochemical gradient into the cell.

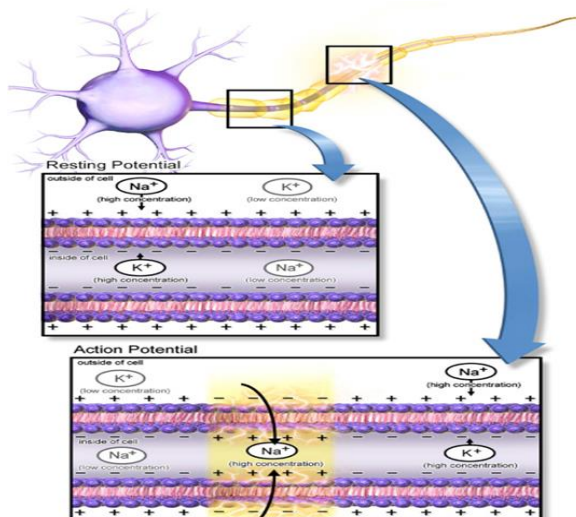


Figure 1.4 Action Potential Propagation Along Axon [Original file]

1.5.3 Stages of the Action Potential

1. Depolarization: A stimulus starts the depolarization of the membrane. Depolarization, also referred to as the upswing, is caused when positively charged sodium ions rush into a nerve cell. As these positive ions rush in, the membrane of the stimulated cell reverses its polarity so that the outside of the membrane is negative relative to the inside [6].

2. Repolarization: Once the electric gradient has reached the threshold of excitement, the “downswing” of repolarization begins. The channels that let the positive sodium ion channels through close up, while channels that allow positive potassium ions open, resulting in the release of positively charged potassium ions from the neuron. This expulsion acts to restore the localized negative membrane potential of the cell, bringing it back to its normal voltage [6].

3. Refractory Phase: The refractory phase takes place over a short period of time after the depolarization stage. Shortly after the sodium gates open, they close and go into an inactive conformation. The sodium gates cannot be opened again until the membrane is repolarized to its normal resting potential. The sodium potassium pump returns sodium ions to the outside and potassium ions to the inside. During the refractory phase this particular area of the nerve cell membrane cannot be depolarized. Therefore, the neuron cannot reach action potential during this “rest period.” This process of depolarization, repolarization, and recovery moves along a nerve fiber from neuron to neuron like a very fast wave. While an action potential is in progress, another cannot be generated under the same conditions. In unmyelinated axons (axons that are not covered by a myelin sheath), this happens in a continuous fashion because there is voltage gated channels throughout the membrane. In myelinated axons (axons covered by a myelin sheath), this process is described as saltatory because voltage-gated channels are only found at the nodes of Ranvier, and the electrical events seem to “jump” from one node to the next. Saltatory conduction is faster than continuous conduction. The diameter of the axon also makes a difference, as ions diffusing within the cell have less resistance in a wider space [6]. Damage to the myelin sheath from disease can cause severe impairment of nerve-cell function. In addition, some poisons and drugs interfere with nerve impulses by blocking sodium channels in nerves.

1.6 SYNAPSES

The locations of such near-contacts are called synapses. The space between the pre-synaptic and post-synaptic membranes is called the synaptic cleft. When an action potential arrives at an axon terminal, it predominately causes the release of a chemical called a neurotransmitter. who diffuses across the synaptic cleft to the post-synaptic membrane, where it binds to specialized receptors and leads to the opening of ion channels, therefore affecting the membrane potential of the post-synaptic neuron. Different classes of neurons release different neurotransmitters such as :

1. First type of neurotransmitter is glutamate. Where glutamate binds to a receptor, the effect is a depolarization of the post-synaptic membrane, i.e., a rise in the membrane potential of the post-synaptic neuron. Therefore one calls glutamate an excitatory neurotransmitter. Two important glutamate receptor classes are the AMPA receptors and the NMDA receptors. They derive their names from synthetic substances that can (artificially) activate them: α -amino-3-hydroxy-5-methyl-4-isoxazolepropionic acid, or AMPA, and N-methyl-D-aspartate, or NMDA. Both AMPA and NMDA receptors are ionotropic, which means that the receptor itself is an ion channel which opens when glutamate binds to it. Both are non-specific cation (positive ion) channels, i.e., they allow various different positive ions (sodium, potassium, and calcium) to pass.

2. A second important neurotransmitter is GABA (gamma-aminobutyric acid). It is usually inhibitory, when it binds to a receptor, the effect is a hyperpolarization of the post-synaptic membrane. GABA acts on various types of GABA receptors.

- a) GABAA receptors are chloride channels that open up when GABA binds to them. Since chloride is more plentiful in the extracellular fluid than in the cell interior, the opening of chloride channels leads to an influx of chloride, and since chloride carries negative charge, this may result in the hyperpolarization of the post-synaptic cell.
- b) GABAB receptors, unlike the other receptors we have mentioned, are metabotropic, not ionotropic. This means that they are not ion channels. Instead, when GABA binds to a GABAB receptor, a signaling cascade, called a second messenger cascade, is set in motion that indirectly leads to the opening of potassium channels. This lead to the flow of potassium out of the post-synaptic cell, and thereby in the hyperpolarization of the cell.

The action potential-triggered release of neurotransmitters is a major mechanism of neuronal communication in the brain. It is called synaptic or chemical communication.

A second important signaling mechanism includes gap junctions that means locations at which neuronal membranes are in contact, with openings in both membranes allowing the direct flow of ions from one neuron into the other. This kind of neuronal communication is called gap-junctional or electrical [7].

Theoretical Background

2.1 Electrical Properties of Neurons

Neurons are filled with a large variety of ions and molecules. Most of these ions carry positive or negative charges. Most of the time, there is an excess concentration of negative charge inside a neuron. The cell membrane is a lipid bilayer that is essentially impermeable to most charged molecules. This insulating feature causes the cell membrane to act as a capacitor by separating the charges lying along its interior and exterior surfaces. Most ion-conducting channels are inside the cell membrane [8].

2.1.1 Ion Channels

Ion channels are proteins in the cell membrane with a hydrophilic pore that facilitates transport of ions across the membrane. The size of the ion channel pore and the charge of amino acids near the opening of the pore help exclude entry of some ions while the entry of others. They classify ion channel upon a selective permeability to different ions. Most ion channels are classified according to the nature of their gating and their selectivity of ions. Ion channels classified by gating are the ligand-gated and voltage-gated ion channels. The most common ligand-gated ion channels are found at the post-synaptic membrane of neurons include NMDA, kainate, AMPA, and GABAA receptors and change conformation when a ligand binds to them. The second class of ion channels, voltage-gated ion channels, undergo conformational changes corresponding to alterations in membrane potential. Voltage-gated ion channels can show selectivity for sodium, potassium, or calcium [9].

1. voltage-gated potassium channels (K_v channels)

K_v channels generally gate between two conformations—an open conformation permeable to potassium and a closed conformation impermeable to potassium.

2. voltage-gated sodium channels (Na_v channels)

often gate between three stable conformations—an open conformation permeable to sodium, a closed conformation impermeable to sodium, and an inactive conformation also impermeable to sodium. Although both the inactive and closed states of Na_v channels are impermeable to sodium, they represent different conformational states of the channel and have different kinetics

2.2.1 Ion Pumps

The membrane also contains selective pumps that expend energy to maintain differences in the concentrations of ions inside and outside the cell such as sodium- potassium pump [8].

2.3.1 Membrane Potential

The potential of the extracellular fluid outside a neuron is defined to be 0. When a neuron is inactive, the excess internal negative membrane potential charge causes the potential inside the cell membrane to be negative. This potential is an equilibrium point at which the flow of ions into the cell matches that out of the cell. The potential can change if the balance of ion flow is modified by the opening or closing of ion channels. Under normal conditions, neuronal membrane potentials vary over a range from about -90 to +50 mV. The order of magnitude of these potentials can be estimated from basic physical principles [8].

2.2 How to Model Neurons?

Neuronal modelling is the process by which a biological neuron is represented by a mathematical structure that includes its biophysical and geometrical characteristics. This structure is referred to as the mathematical model or the model of the neuron. The behavior of this representation may serve a number of purposes: for example, it may be used as the basis for estimating the biophysical parameters of real neurons or it may be used to define the computational and information processing properties of a neuron. Neuronal modelling requires not only an understanding of mathematical and computational techniques, but also an understanding of the what the process of modelling entails [10].

2.1.2 Spiking Neuron Models

There are two factors that can characterize each spiking neuron model:

1. Biologically plausible: this means that the spiking neuron will be able to produce a set of firing patterns or behaviors exhibited by real biological neurons.

2. Computational efficiency: this factor is determined by the number of variables used in order to represent the neuron model (activation function) and the number of floating point operations needed to accomplish one mille second (ms) of model simulation. These operations affect the time needed to accomplish the simulation, as well as it affect computational resources such as processing units and memory usage. The model that has less number of variables and floating point operations is more efficient [11].

2.2.2 Spiking Neurons Can Be Simulated Using Various Models:

1. The Hodgkin-Huxley Model
2. Reduced Traub-Miles Model of a Pyramidal Neuron in Rat Hippocampus
3. Wang-Buzsáki Model of an Inhibitory Interneuron in Rat Hippocampus
4. Erisir Model of an Inhibitory Interneuron in Mouse Cortex
5. Izhikevich Model

2.3 Hodgkin and Huxley Model

In the 1940s, Alan Hodgkin and Andrew Huxley explain the fundamental physical mechanism by which electrical impulses are generated by nerve cells, and travel along axons, in animals and humans. They are experimented with isolated pieces of the giant axon of the squid. They are summarized their conclusions in a series of publications in 1952; the last of these papers [12] is arguably the single most influential paper ever written in neuroscience, and forms the foundation of the field of mathematical and computational neuroscience.

the model assumes that action potential generation in neurons is mainly performed by the electrical properties of the cell membrane. Several factors provide to the electrical properties of the cell membrane. For instance, ion channels such as Nav, Kv, and leak channels span the membrane and selectively pass ions across it. The voltage-gated channels are represented in Figure 2.1 as variable resistors (the resistors with a pointer going through them) because the amount of resistance to flow depends on the membrane potential, whereas the leak channel, which has a constant resistance to ion flow, is represented by an ordinary resistor. The model represents the Nernst potential that is generated by the difference in ion concentration for each ion as a battery. Notice that current flows from the inside of the cell (at the top of the electrical circuit) to the outside of the cell by either inducing a charge buildup at the membrane (represented by the capacitor) or by flowing through one of the three ion channels present in the membrane. From simple electrical circuit theory, you can represent the following circuit using a set of equations [9].

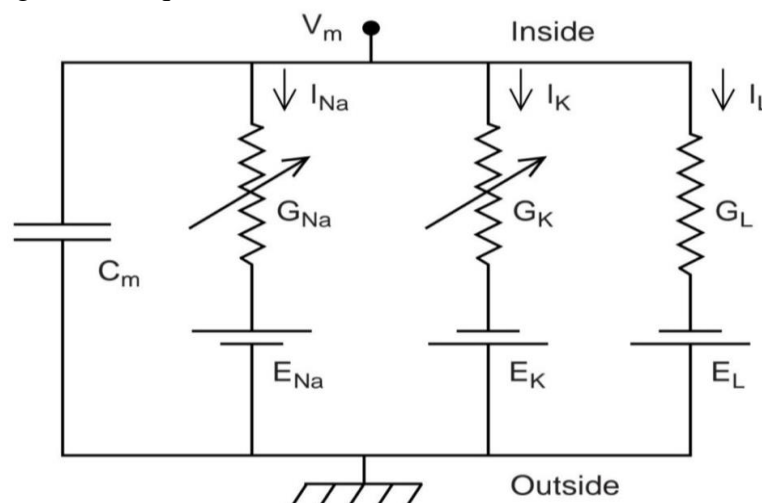


Figure 2.1 An electrical circuit diagram of a single axonal compartment of a neuron [9]

HH model describes how the membrane potential charges over time in a small region of squid giant axon. Hodgkin and Huxley tie a silver wire lengthwise through the axon, therefore ending spatial variations in the membrane potential v . This is called the space clamp technique. and summarize the mechanism in the form of a system of ordinary differential equations 4 (ODEs). A nerve cell membrane acts like a capacitor, separating two charge layers of opposite signs according to the fundamental equation of a capacitor [7].

$$Cv = Q \quad (2.1)$$

where Q is the separated charge, v is the membrane potential, C is the capacitance. If Q and v depend on time, t , we can differentiate both sides of above equation.

$$C \frac{dv}{dt} = I_{total}, \quad (2.2)$$

where $I_{total} = \frac{dQ}{dt}$ is the total electrical current from one side of the capacitor to the other; this equation is the starting point for the Hodgkin-Huxley ODEs. Total current I was made up of four components: A sodium current I_{Na} , a potassium current I_K , a small additional current which they called the leak current and denoted by I_L , carried by chloride and other ions, and the current I that they themselves injected, using electrodes.

$$C \frac{dv}{dt} = I_{Na} + I_K + I_L + I \quad (2.3)$$

The currents I_{Na} , I_K , and I_L are assumed to obey Ohm's law

$$I_{Na} = g_{Na}(v_{Na} - v), \quad I_K = g_K(v_K - v), \quad I_L = g_L(v_L - v).$$

v_{Na} and v_K are the Nernst potentials of sodium and potassium, the leak current is a mixture of ion species, v_L is a weighted average of the Nernst potentials of those ion species.

Nernst equation

$$v_X = \frac{KT}{zq} \ln \frac{[X]_{ex}}{[X]_{in}} \quad (2.4)$$

At human body temperature

$$\frac{KT}{q} \approx 26.7mV$$

Hodgkin and Huxley derive from their experiments that, and how, the conductances g_{Na} and g_K track changes in cell voltage

$$g_{Na} = g_{Na} m^3 h \quad g_K = g_K n^4 \quad (2.5)$$

Where g_{Na} and g_K are constant conductances, and m , h , and n are time-dependent dimensionless quantities varying between 0 and 1. Hodgkin and Huxley are proposed a mathematical description of their observations. They introduce additional "gating" variables m , h and n to model the probability that a channel is open at a given moment in time. The combined action of m and h controls the Na^+ channels while the K^+ gates are controlled by n . For example, the effective conductance of sodium channels is modeled as $\frac{1}{R_{Na}} = g_{Na} m^3 h$, where m describes the activation (opening) of the channel and h its inactivation (blocking). The conductance of potassium is $\frac{1}{R_K} = g_K n^4$, where n describes the activation of the channel. In the Hodgkin-Huxley model, m , h , and n obey simple first-order ODEs of the form [7].

$$\frac{dm}{dt} = \frac{m_{\infty}(v) - m}{\tau_m(v)} \quad \frac{dh}{dt} = \frac{h_{\infty}(v) - h}{\tau_h(v)} \quad \frac{dn}{dt} = \frac{n_{\infty}(v) - n}{\tau_n(v)} \quad (2.6)$$

where m_{∞} , τ_m , h_{∞} , τ_h , n_{∞} , and τ_n are functions of v . Instead of explicitly spelling out the three equations for m , h , and n , we will from now on briefly write

$$\frac{dx}{dt} = \frac{x_{\infty}(v) - x}{\tau_x(v)} \quad \text{for } x=m, n, h. \quad (2.7)$$

In the Hodgkin-Huxley model, action potentials are generated when the m -gates open up in response to an initial depolarization, causing a sodium current into the cell. This sodium current raises v further, and a sort of chain reaction ensues. The rise in v is terminated when the h -gates close, thereby ending the inflow of sodium, and the n -gates open, leading to an outflow of potassium. It is crucial here that τ_m is much smaller than τ_h and τ_n , see Fig(3.1) . If the time constants were all equal, the closing of the h -gates and the opening of

the n-gates could cancel the opening of the m-gates immediately, thereby preventing the voltage spike. If x_∞ and τ_x are constants, independent of v , (2.7) will be equivalent to

$$x(t) = x(0)e^{-t/\tau_x} + x_\infty(1 - e^{-t/\tau_x}) \quad (2.8)$$

You can drive (2.8) from (2.7) by using separation of variables.

$$\frac{dx}{dt} = \frac{x_\infty - x}{\tau_x} \implies \frac{dx}{x_\infty - x} = \frac{1}{\tau_x} dt$$

$$-\ln = (x_\infty - x) = \frac{1}{\tau_x} t + c$$

$$x_\infty - x = e^{-\frac{t}{\tau_x} + c} \dots\dots\dots(a)$$

$$c = x_\infty - x(0) - e^{-\left(\frac{0}{\tau_x}\right)} \quad \text{by assume } t=0$$

$$c = x_\infty - x(0) - 1 \dots\dots\dots(b)$$

By substituting equation (b) into equation (a)

$$x_\infty - x = e^{-\frac{t}{\tau_x} + [x_\infty - x(0) - 1]}$$

$$x(t) = -e^{-\frac{t}{\tau_x} - 2x_\infty + x(0) + 1} \quad \text{by assume } x=x(0)$$

$$x(t) = x(0)e^{-\frac{t}{\tau_x}} + x_\infty(1 - e^{-\frac{t}{\tau_x}})$$

The weight multiplying $x(0)$ starts out, at $t = 0$, at 1, and decays to 0 exponentially fast. The weight multiplying x_∞ starts out at 0, and converges to 1 exponentially fast. Thus $x(t)$ moves from $x(0)$ to x_∞ (its limit as $t \rightarrow \infty$) exponentially fast. The time it takes for $x(t)$ to make “substantial progress” towards x_∞ , namely, the time it takes for the weight in front of $x(0)$ to decay by a factor of $1/e$, is τ_x . We say that $x(t)$ converges to x_∞ exponentially with time constant τ_x . Thus eqs. (3.5) express that m , h , and n move towards m_∞ , h_∞ , and n_∞ , exponentially with time constants τ_m , τ_h , and τ_n . Note, however, that m_∞ , h_∞ , and n_∞ are “moving targets” — they change as v changes. How quickly m , h , and n respond to changes in v , and therefore in m_∞ , h_∞ , and n_∞ , is measured by τ_m , τ_h , and τ_n . The functions $x_\infty(v)$ and $\tau_x(v)$, $x = m, h, n$, are defined by Hodgkin and Huxley so that the resulting ODEs will match their experimental data. Figure 3.1 in chapter 3 shows the graphs of these functions. We summarize the Hodgkin-Huxley model of the space-clamped squid axon:

$$C \frac{dv}{dt} = g_{Na} m^3 h (v_{Na} - v) + g_K n^4 (v_K - v) + g_L (v_L - v) + I \quad (2.9)$$

$$\frac{dx}{dt} = \frac{x_\infty(v) - x}{\tau_x(v)} \quad \text{for } x=m, n, h. \quad (2.10)$$

This is a system of four ODEs for the four unknown functions v , m , h , and n . Up to now, we have thought of C as capacitance, g_{Na} , g_K , and g_L as conductances, and I as a current. However, dividing both sides of (2.9), by the total membrane area. All that is left to do to specify the model completely is to specify the constants C , v_{Na} , v_K , v_L , g_{Na} , g_K , and g_L , and the formulas for $x_\infty(v)$ and $\tau_x(v)$, $x = m, h, n$. The constants are

Table (2.1) constant of Hodgkin-Huxley Model [7]

C	v_{Na}	v_K	v_L	g_{Na}	g_K	g_L
1 $\mu\text{F}/\text{cm}^2$	45 mV	-82 mV	-59 mV	120 mS/cm ²	36 mS/cm ²	0.3 mS/cm ²

Note that g_L is very much smaller than g_{Na} and g_K . Nonetheless the leak conductance is crucial for the behavior of the model. The reason is that between voltage spikes, g_L is not very small in comparison with $g_{Na}m^3h$ and g_Kn^4 . Sodium and potassium channels are largely closed between voltage spikes, while the leak channels remain open. We now specify $x_\infty(v)$ and $\tau_x(v)$, $x = m, h$ and n . First, we observe that (2.7) can be re-written in the form

$$\frac{dx}{dt} = \alpha x(v)(1 - x) - \beta x(v)x. \quad (2.11)$$

The relation between the parameters x_∞ and τ_x in (3.6), and the parameters αx and βx in (3.10), is

$$x_{\infty} = \frac{\alpha_x}{\alpha_x + \beta_x} \qquad \tau_x = \frac{1}{\alpha_x + \beta_x} \qquad (2.12)$$

or, equivalently

$$\alpha_x = \frac{x_{\infty}}{\tau_x} \qquad \beta_x = \frac{1 - x_{\infty}}{\tau_x} \qquad (2.13)$$

Presence gates guarding channels as before, and assuming that open gates close and closed gates open at random times, with time rates dependent on v , you can explain α_x as the time rate at which closed gates open, and β_x as the time rate at which open gates close. That is, in a short time Δt , the probability that a closed gate opens is approximately $\alpha_x \Delta t$, and the probability that an open gate closes is approximately $\beta_x \Delta t$. The differential equation governing x can be described either by specifying x_{∞} and τ_x , or equivalently by specifying α_x and β_x . Hodgkin and Huxley measure the quantities x_{∞} and τ_x and compute from them the time rates α_x and β_x (measured in ms^{-1}) as functions of v (measured in mV). It is easier to fit α_x and β_x with simple formulas than to fit x_{∞} and τ_x directly, because all α_x and β_x are monotonic functions of v , while the τ_x are not. Up to notation, Hodgkin and Huxley's formulas are

$$\alpha_m(v) = \frac{(v + 45)/10}{1 - \exp(-(v + 45)/10)}, \qquad \beta_m(v) = 4 \exp(-(v + 70)/18)$$

$$\alpha_h(v) = 0.07 \exp(-(v + 70)/20), \qquad \beta_h(v) = \frac{1}{\exp(-(v + 40)/10) + 1},$$

$$\alpha_n(v) = \frac{1}{100} \frac{v + 60}{1 - \exp(-(v + 60)/10)}, \qquad \beta_n(v) = \frac{1}{8} \exp(-(v + 70)/80).$$

2.4 Activation, Inactivation, De-activation, and De-inactivation

In Hodgkin-Huxley-like models, a gating variable x is generally called an activation variable if x_{∞} is an increasing function of v , and an inactivation variable if x_{∞} is a decreasing function of v . As mentioned earlier, in the classical Hodgkin-Huxley model, m and n are activation variables, and h is an inactivation variable. An increase in an activation variable as a result of depolarization causes activation of the current. A decrease in an activation variable as a result of hyperpolarization causes de-activation of the current. A decrease in an inactivation variable as a result of depolarization causes inactivation, and an increase in an inactivation variable as a result of hyperpolarization causes de-inactivation of the current. Note in particular that de-activation is not the same as inactivation, and de-inactivation is not the same as activation. We also sometimes use the word "induced." For instance, a current with an inactivation gate that is de-inactivated in response to hyperpolarization might be called "hyperpolarization-induced." A current with an activation gate that is activated in response to firing might be called 'firing-induced' [7].

2.5 MATLAB Software

MATLAB (matrix laboratory) is a multi-paradigm numerical computing environment and proprietary programming language developed by Math Work. MATLAB allow matrix manipulation, plotting of functions and data, implementation of algorithms, creation of user interface and interfacing with programs written in faces and inter facing with programs written in other language, including c, cc++, c#, Java, Fortan and Python. Although MATLAB is intended primarily for numerical computing, an optional toolbox uses the MuPAD symbolic engine, allowing access to symbolic computing abilities.

2.5.1 Solving Differential Equations Numerically

The current-voltage properties of an ion channel depend on solve an ordinary differential equation. As it describes the probability of the channel being open given the initial condition that $P_o(0) = 0$. In general, solving differential equations can be very tricky (if not impossible), There are some ways to simplify solutions whereas the simplest method for approximating the solution to a differential equation is Euler's method [9]. It is based on the definition of the derivative:

$$\frac{df}{dx} = \lim_{\Delta x \rightarrow 0} \frac{f(x + \Delta x) - f(x)}{\Delta x} \quad (2.14)$$

2.5.2 Euler Method

The Euler method is the simplest numerical integration method to solve ordinary differential equations. In practice, the Euler method is very quick to compute but prone to instability and inaccuracy. The differential equation $y'(t) = f(t, y(t))$ where the initial condition is $y(t_0) = y_0$ and the value of t_n is defined to be $t_0 + n \cdot h$ where h is the size of the step, can be solved at t_n using the Euler method. The Euler method yields the result $y_{n+1} = y_n + h \cdot f(t_n, y_n)$. The code for implementing Equations of Hodgkin-Huxley model are not very complicated. You can solve them using Euler's method. The Euler method is a quick and easy method used to estimate a function from its ordinary differential equation (ODE). It is a step-wise calculation based on the idea that the tangents, if close enough, can provide an estimate of the unknown function. In simple terms to solve a differential equation with the Euler method [13]:

1. Calculate starting values based on prior knowledge
2. Calculate the differential equation, using values obtained in step 1 (or step 4 if repetition)
3. Multiple results from step 2 by a small time step, dt (often 0.1 or 0.01)
4. Add values obtained from step 3 to the starting values used in step 2
5. Repeat steps 2 to 4

2.6 A Discussion of Some Simple Models Neurons in Rodent Brains

Some models are discussed here such as RTM model, WB, and Erisir models. All of these three models are a form of the classical Hodgkin-Huxley model eqs (2.9) and (2.10) but with different parameter values, different functions α_x and β_x (remember that α_x and β_x determine the functions x_∞ and τ_x), and with the assumption that " $\tau_m = 0$," that is, $m = m_\infty(v)$. Thus m is not a dependent variable any more, but a direct function of v . This assumption is justified by the fact that but with different parameter values, different functions α_x and β_x (remember that α_x and β_x determine the functions x_∞ and τ_x), and with the assumption that $\tau_m = 0$ that is, $m = m_\infty(v)$. Thus m is not a dependent variable any more, but a direct function of v . This assumption is justified by the fact that [7].

$$\tau_m(v) = \frac{1}{\alpha_m(v) + \beta_m(v)} \quad (2.15)$$

is very small for all v ; see The graphs of the functions x_∞ and τ_x for all three models are given in Fig 3.3, and the constants in Table 2.1.

Table (2.2) Constants in the three Hodgkin-Huxley-like models [7]

	C	vNa	vk	vl	gNa	gk	gl
RTM	1	50	-100	-67	100	80	0.1
WB	1	55	-90	-65	35	9	0.1
Erisir	1	60	-90	-70	112	224	0.5

2.6.1 Reduced Traub-Miles Model of a Pyramidal Neuron in Rat Hippocampus.

This is a slight modification of a model due to Ermentrout and Kopell which also is a substantial simplification of a model of a pyramidal excitatory cell in rat hippocampus due to Traub and Miles. The constants are specified in Table 5.1[7]. The functions α_x and β_x are

$$\alpha_m(v) = \frac{0.32(v + 54)}{1 - \exp(-(v + 54)/4)}, \quad \beta_m(v) = \frac{0.28(v + 27)}{\exp((v + 27)/5) - 1}$$

$$\alpha_h(v) = 0.128 \exp(-(v + 50)/18), \quad \beta_h(v) = \frac{4}{1 + \exp(-(v + 27)/5)},$$

$$\alpha_n(v) = \frac{0.032(v + 52)}{1 - \exp(-(v + 52)/5)}, \quad \beta_n(v) = 0.5 \exp(-(v + 57)/40).$$

The red, solid curves in Fig. 3.3 show the graphs of x_∞ and τ_x , $x = m, h, \text{ and } n$. Figure 3.4 shows a voltage trace with $I = 1.5 \mu\text{A}/\text{cm}^2$

2.6.2 Wang-Buzsáki Model of an Inhibitory Interneuron in Rat Hippocampus

Wang and Buzsáki propose a model of an inhibitory basket cell in rat hippocampus. Basket cells derive their name from the fact that the branches of their axonal arbors form basket-like structures surrounding the cell bodies of other cells. Two different classes of inhibitory basket cells are ubiquitous in the brain, the parvalbumin-positive (PV+) basket cells, which contain the protein parvalbumin, and the cholecystokinin-positive (CCK+) basket cells [55], which contain the hormone cholecystokinin. The PV+ basket cells are called fast-firing because they are capable of sustained high-frequency firing, and are known to play a central role in the generation of gamma frequency (30–80 Hz) oscillations. It is thought that gamma rhythms are important for sensory processing, attention, and working memory. The WB model is patterned after the fast-firing PV+ basket cells. For the constants, see Table 2.1 . The functions αx and βx are:

$$\alpha_m(v) = \frac{0.1(v + 35)}{1 - \exp(-(v + 35)/10)}, \quad \beta_m(v) = 4 \exp(-(v + 60)/18),$$

$$\alpha_h(v) = 0.35 \exp(-(v + 58)/20), \quad \beta_h(v) = \frac{5}{1 + \exp(-0.1(v + 28))},$$

$$\alpha_n(v) = \frac{0.05(v + 34)}{1 - \exp(-0.1(v + 34))}, \quad \beta_n(v) = 0.625 \exp(-(v + 44)/80).$$

The blue dash-dotted curves in Fig 3.3 show the graphs of x_∞ and τ_x $x=m, h$ and n . Figures (3.7),(3.8),(3.9) shows a voltage trace with $I=0.75 \mu\text{A}/\text{cm}^2$. The most striking difference between Figs (3.3)and (3.7),(3.8),(3.9) is that the spike after hyperpolarization, so the hyperpolarization following an action potential, is far less deep in the WB model than in the RTM model. The spike after hyperpolarization is less pronounced for the WB model than for the RTM model because the maximal conductance densities g_{Na} and g_K are small. Deeper after hyperpolarization be obtain if g_{Na} and g_K are raises or h and n make slower [7].

2.6.3 Erisir Model of an Inhibitory Interneuron in Mouse Cortex

Erisir et al. proposes a model of an inhibitory interneuron in mouse somatosensory cortex., the model takes the same form as the RTM and WB models, except that the potassium conductance is g_{Kn}^2 , not g_{Kn}^4 . For the constants, see Table(2.1). The functions αx and βx are

$$\alpha_m(v) = \frac{40(75.5 - v)}{\exp((75.5 - v)/13.5) - 1}, \quad \beta_m(v) = 1.2262 \exp(-v/42.248),$$

$$\alpha_h(v) = 0.0035 \exp(-v/24.186), \quad \beta_h(v) = \frac{-0.017(v + 51.25)}{\exp(-(v + 51.25)/5.2) - 1},$$

$$\alpha_n(v) = \frac{95 - v}{\exp((95 - v)/11.8) - 1} \quad \beta_n(v) = 0.025 \exp(-v/22.222)$$

Note that g_{Na} and g_K are quite large in the Erisir model, even larger than in the RTM model. As a result, the voltage rises almost to v_{Na} during an action potential, and falls almost to v_K immediately following an action potential. The leak conductance density g_L is large as well. That we use g_{kn}^2 instead g_{kn}^4 whith Figures 3.10, 3.,11 and 3.13. Using g_{Kn}^2 instead of g_{Kn}^4 has the following effects, which one can see when comparing Figs. 3.10 and 3.13.

2.7 Simplified Model of Spiking Neurons

Understanding how different areas of the brain interact with each other to perform higher level functions such as motor coordination and speech is a major interest of modern neuroscience but also an extremely difficult one. Many factors contribute to the global dynamics of neural networks. First, neurons

isolated from a network exhibit a variety of patterns and behaviors. Some of these behaviors are more common than others. For example, under normal conditions there are more regular spiking neurons in the cortex than intrinsic bursting ones. How these different dynamics are manifested at the network level remains an open area of current research. Second, the synaptic coupling between neurons can have a large impact on the network's dynamics leading to synchronization among the neurons and network oscillations. Network oscillations in the brain are often categorized by their frequency. Oscillations with a frequency less than 4 Hz are called delta rhythms. Oscillations between 4 and 8 Hz are called theta rhythms. Rhythms from 8 to 12 Hz are called alpha rhythms, and rhythms from 12 to 30 Hz are called beta rhythms. Rhythms above 30 Hz are called gamma rhythms[9] . A simple spiking model is presented that is as biologically plausible as the Hodgkin–Huxley model, yet as computationally efficient as the integrate-and-fire model. Depending on four parameters, the model reproduces spiking and bursting behavior of known types of cortical neurons. Mathematical analysis of the model is published in the monograph by Izhikevich. The form presented here is more suitable for large-scale simulations. The model for this section is a two-dimensional system of ordinary differential equations with a reset condition [14].

$$\frac{dv}{dt} = 0.04v^2 + 5v + 140 - u + I \quad (2.16)$$

$$\frac{du}{dt} = a(bv - u) \quad (2.17)$$

The reset condition is:

If: $v \geq 30$ then:

$$\left. \begin{array}{l} v \left\{ \begin{array}{l} c \leftarrow c \\ u \leftarrow u+d. \end{array} \right. \end{array} \right. \quad (2.18)$$

The variable v represents the membrane potential of the neuron while u represents a generic recovery variable that feeds back negatively onto v . There are five additional parameters in the model: I , a , b , c , and d . The parameter I represents external input to the neuron. This input can consider as external input to the neuron from outside the network or even synaptic input from a neuron within the network. The parameter a controls the rate of recovery of u , and b controls the sensitivity of recovery to subthreshold fluctuations of the membrane potential. The parameters c and d control the after-spike reset values for v and u , respectively. If you choose certain parameter combinations, this simple model can exhibit all the firing patterns and behaviors, as shown in figure 3.10 in chapter 3. A complete network of neurons can be modeled through to couple many neurons together where each neuron behaves according to Equations 2.16–2.18. This means that you must specify a value for each parameter for each neuron that you model. He added that since the network is coupled (i.e., the neurons are connected to each other), the input I to a particular neuron will depend on other neurons in the network that synapse onto it. Therefore, you will need to model the connectivity of the network. you will choose to make every neuron in the network be connected to every other neuron in the network, or possibly make neurons connect only to neurons that are close. Additionally, you need to choose whether a connection between neurons will be excitatory or inhibitory and how strong the connection will be. The code for implementing Equations 2.16–2.18 are not very complicated. You can solve them using Euler's method Previously mentioned in section 2.5.1 [9]

Simulation Results

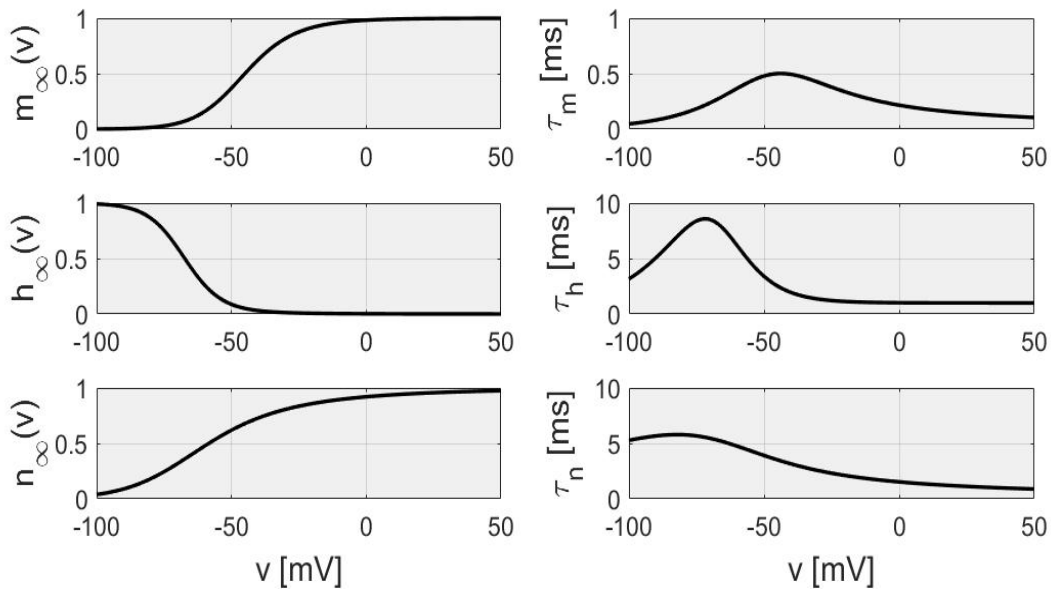


Figure 3.1 The functions $x_{\infty}(v)$ and $\tau_x(v)$ in Hodgkin-Huxley model [7]

In the above Figure are graphs showing functions of $x_{\infty}(v)$ and $\tau_x(v)$ where $x = m, h,$ and n in Hodgkin-Huxley model, so that the results of ODEs match to experimental data. we make a few observations based on the graphs:

1. τ_m is about 10 times smaller than τ_h and τ_n . Therefore m responds to changes in v much faster than h and n . The Hodgkin-Huxley equations are a slow-fast system, that is, there are two significantly different time scales, a slow one and a fast one.
2. m_{∞} and n_{∞} are increasing functions of v . One therefore calls m and n activation variables, as v rises, m -gates open, and so do n -gates, In spite of a ten times slower time scale. Also you can say that the m - and n -gates are activation gates.
3. h_{∞} is a decreasing function of v . One therefore calls h an inactivation variable. As v rises, h -gates close, but ten times slower than m -gates open. Also you can say that the h -gate is an inactivation gate.

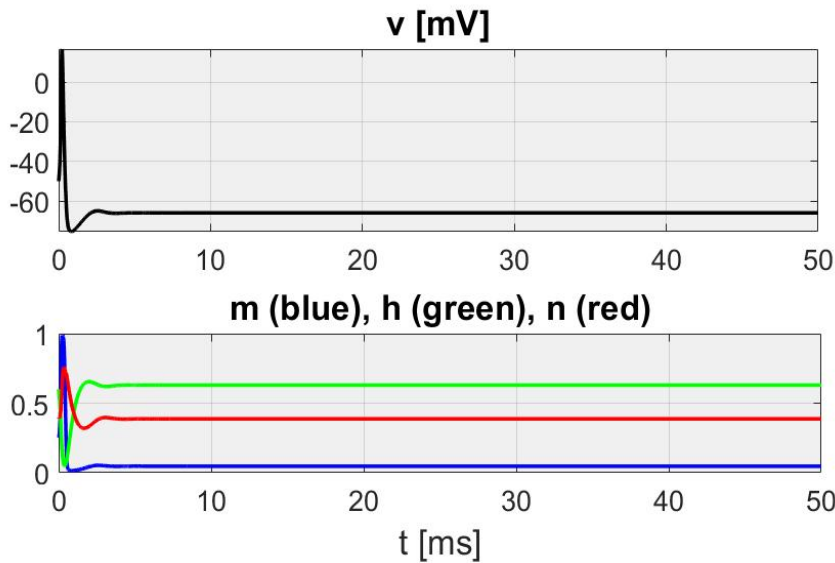


Figure 3.2 A solution of the Hodgkin-Huxley ODEs with $I = 10 \mu\text{A}/\text{cm}^2$ [7].

In Figure above shows an example of a solution Hodgkin-Huxley ODEs in (2.9),(2.10), that indicate an action potential is produced .

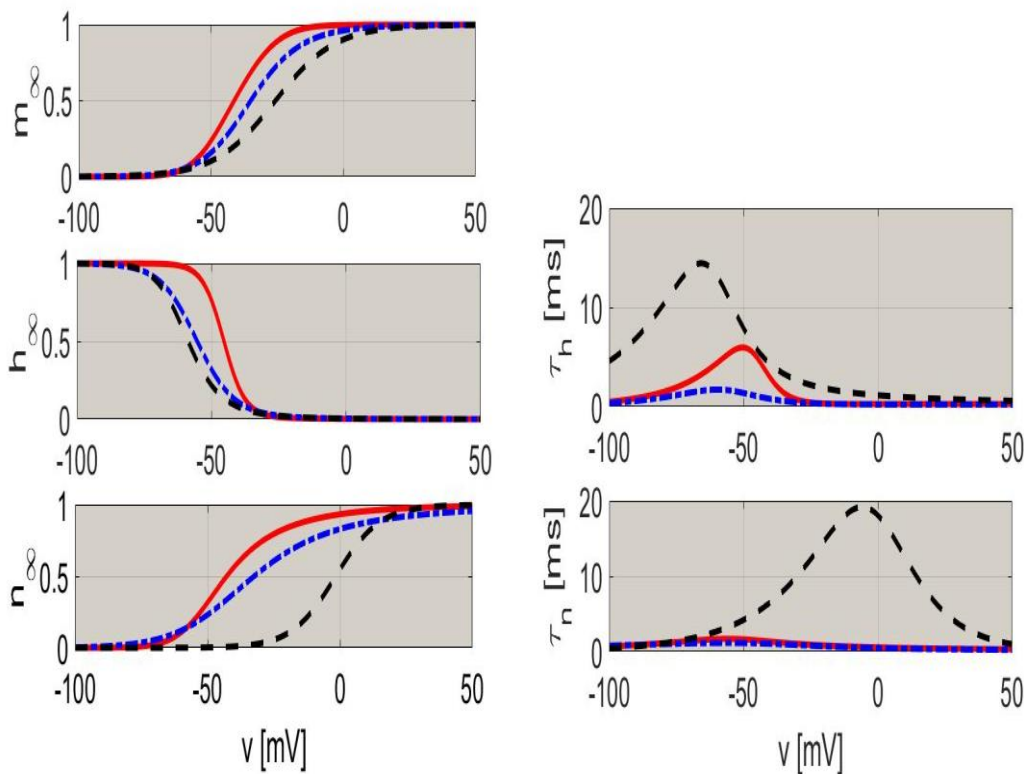


Figure 3.3 The functions x_∞ and τ_x in RTM, WB and Erisir neurons [7]

The Figure above shows the graphs of the functions x_∞ and τ_x for the RTM neuron (red and solid), WB neuron (blue, dash-dots), and Erisir neuron (black, dashes). We leave out τ_m because $m = m_\infty(v)$ in all three of these models.

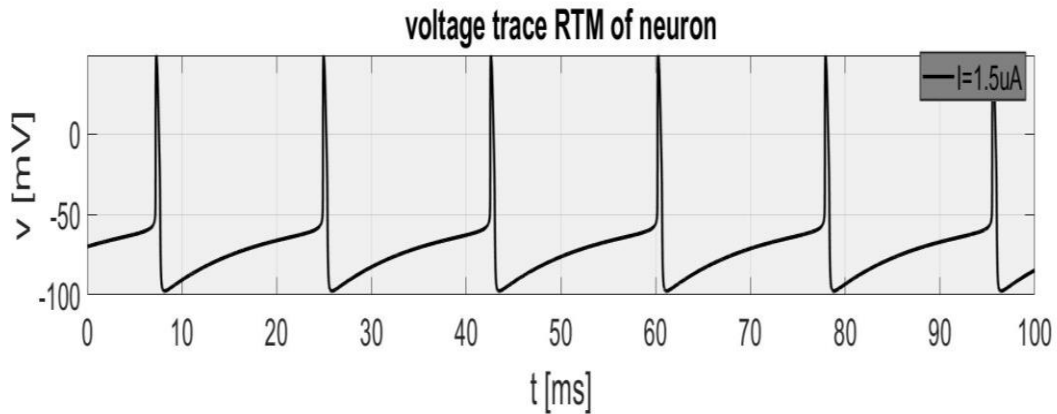


Figure 3.4 Voltage trace of the RTM neuron with $I=1.5\mu\text{A}/\text{cm}^2$ [7]

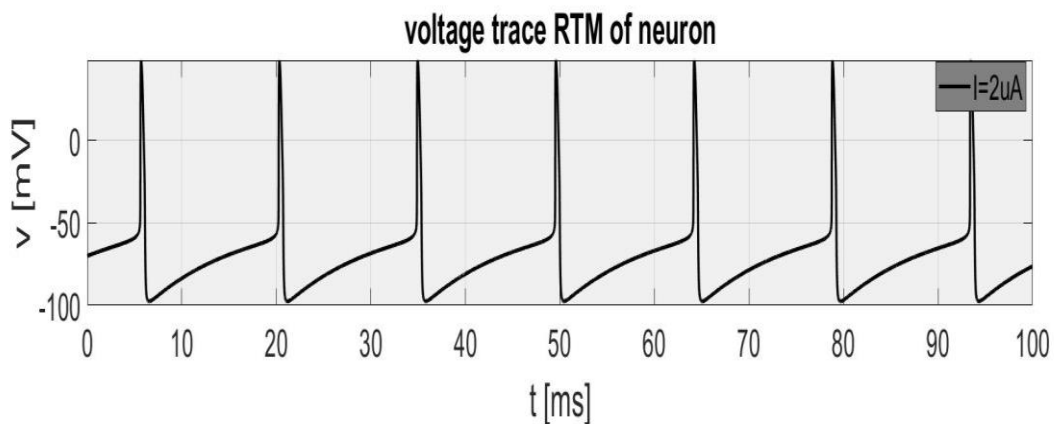


Figure 3.5 Voltage trace of the RTM neuron with $I=2\mu\text{A}/\text{cm}^2$ [7]

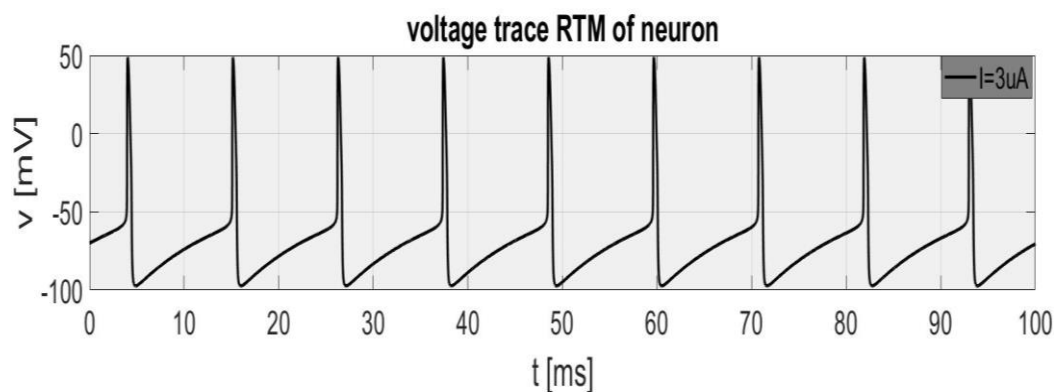


Figure 3.6 Voltage trace of the RTM neuron with $I=3\mu\text{A}/\text{cm}^2$ [7]

In Figures 3.4,3.5 and 3.6 above shows a voltage trace of RTM neuron with $I = 1.5$,2 and $3\mu\text{A}/\text{cm}^2$ respectively. These Figures represent voltage independent time, and each time a different injection current or a stimulate current. This means that by increasing a current, the frequency increases with constant voltage and time values. if the current value is higher than the threshold value for generation the action potential.

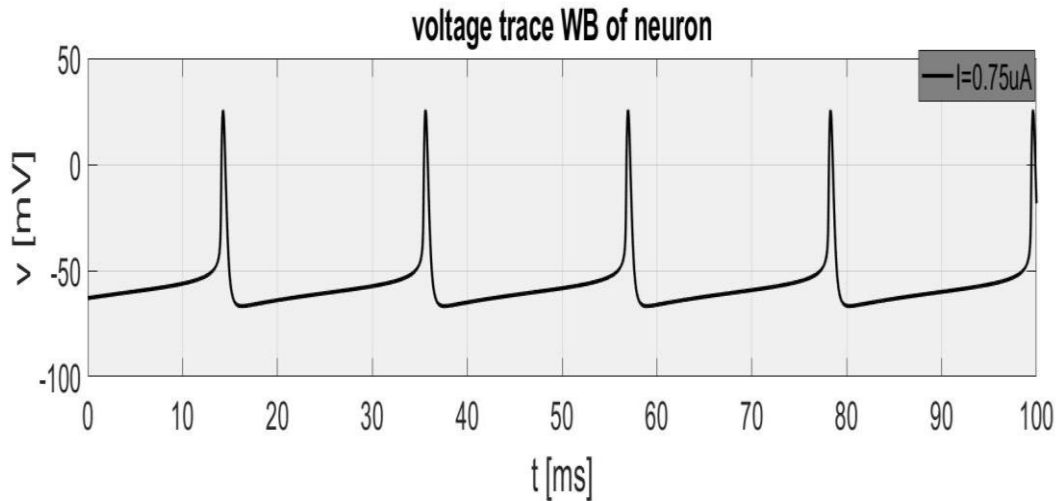


Figure 3.7 Voltage trace of the WB with neuron with $I=1.75\mu\text{A}/\text{cm}^2$ [7]

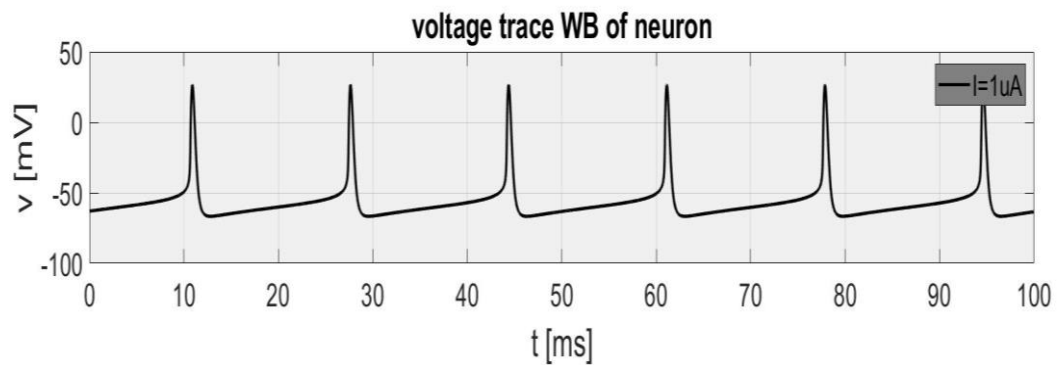


Figure 3.8 Voltage trace of the WB neuron with $I=1\mu\text{A}/\text{cm}^2$ [7]

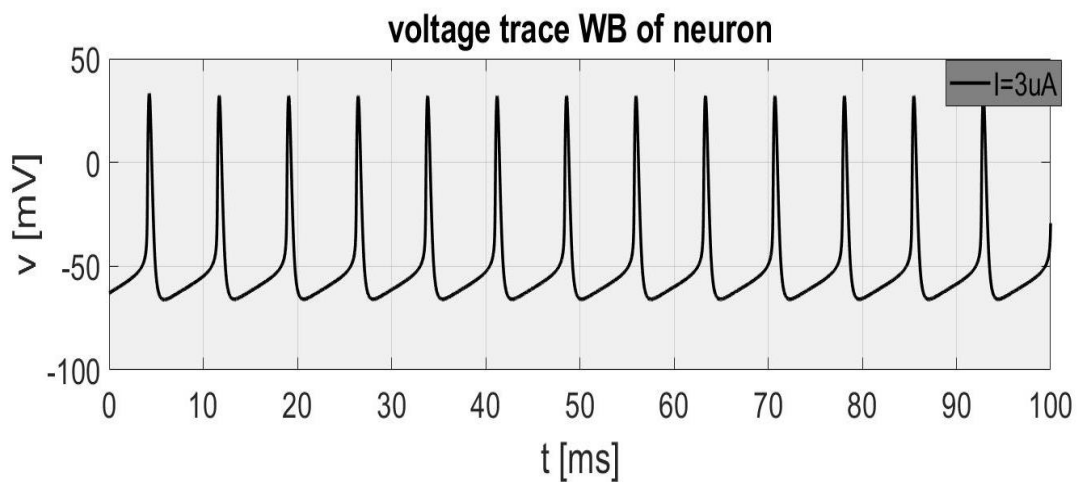


Figure 3.9 Voltage trace of the WB neuron with $I=3\mu\text{A}/\text{cm}^2$ [7]

In Figures 3.7,3.8 and 3.9 above shows a voltage trace with $I = 0.75$,1 and $3\mu\text{A}/\text{cm}^2$ these figures represent voltage independent time, and each time a different injection current or a stimulate current. This means that by increasing a current, the frequency increases with constant voltage and time values. if the current value is higher than the threshold value for generation the action potential.

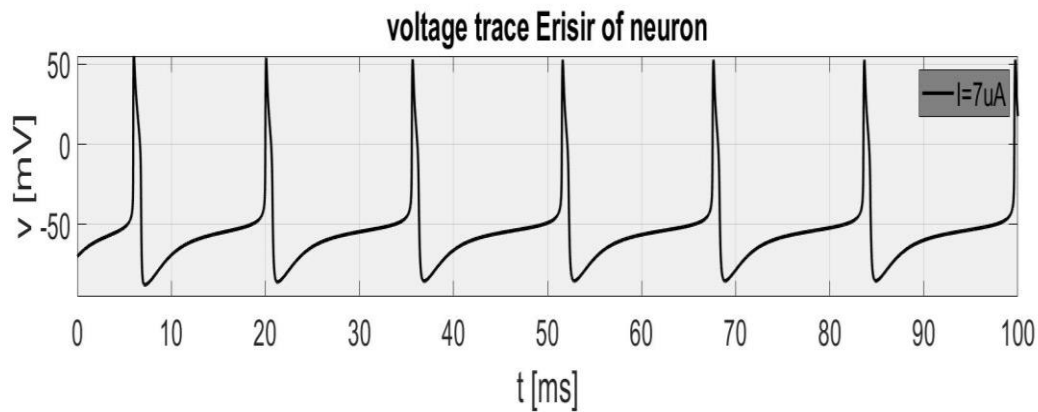


Figure 3.10 Voltage trace of the Erisir neuron with $I = 7\mu\text{A}/\text{cm}^2$ [7]

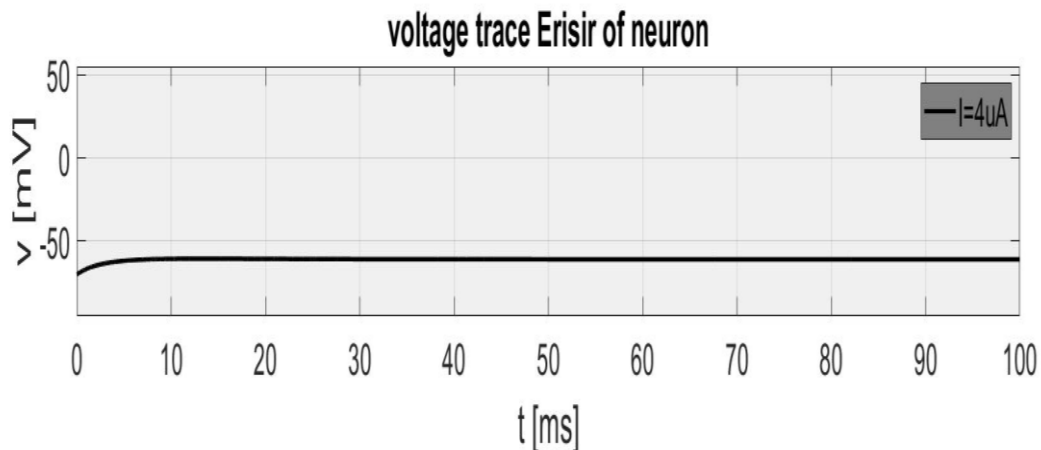


Figure 3.11 Voltage trace of the Erisir neuron with $I = 4\mu\text{A}/\text{cm}^2$ [7]

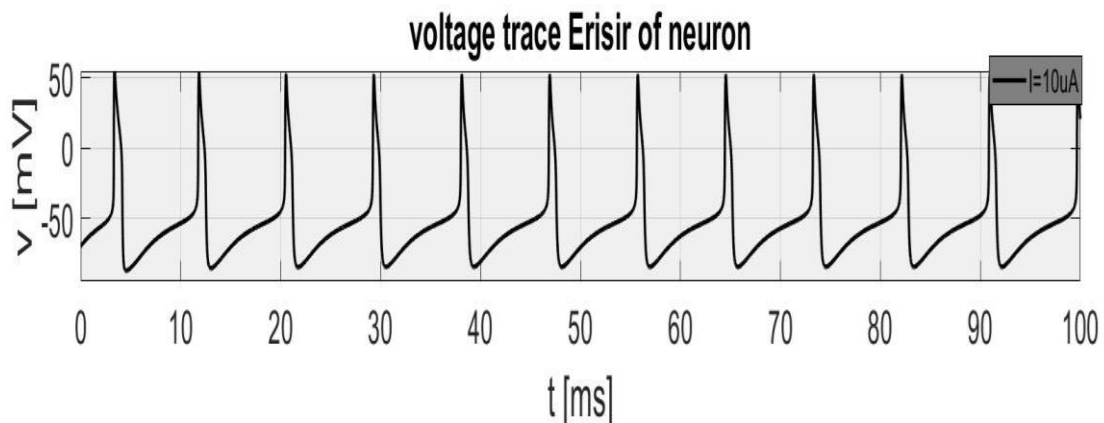


Figure 3.12 Voltage trace of the Erisir neuron with $I = 10\mu\text{A}/\text{cm}^2$ [7]

In Figures 3.10, 3.11 and 3.12 above shows a voltage trace with $I = 7, 4$ and $10 \mu\text{A}/\text{cm}^2$ respectively. These Figures represent voltage independent to time, and each time a different injection current or a stimulate current. This means that by increasing a current, the frequency increases with constant voltage and time values. If the current value is higher than the threshold value for generation the action potential.

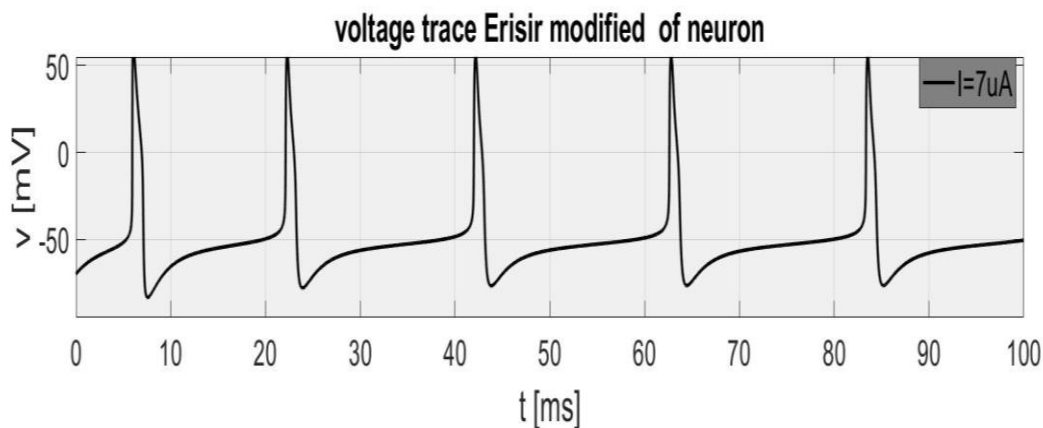


Figure 3.13 Voltage trace of modified Erisir neuron with potassium conductance equal to g_{Kn4} instead of g_{Kn2} , $I = 7 \mu A/cm^2$ [7]

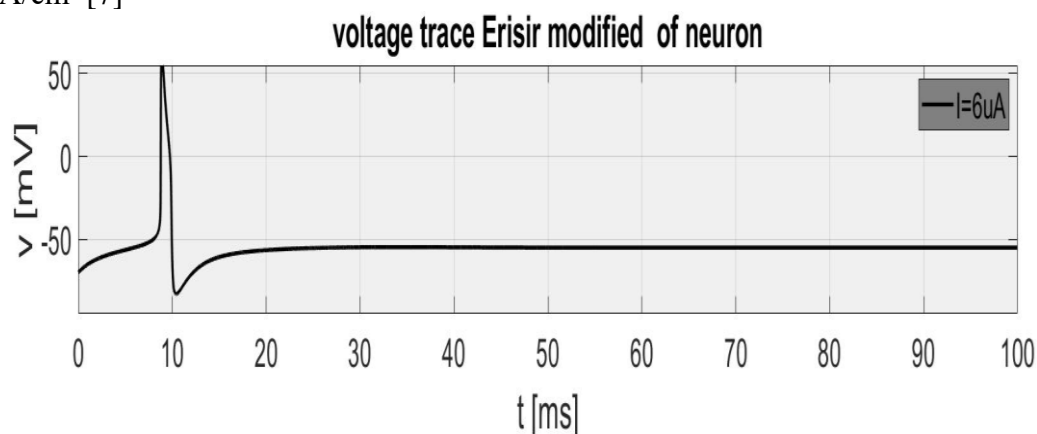


Figure 3.14 Voltage trace of modified Erisir neuron with potassium conductance equal to g_{Kn4} instead of g_{Kn2} , $I = 6 \mu A/cm^2$ [7]

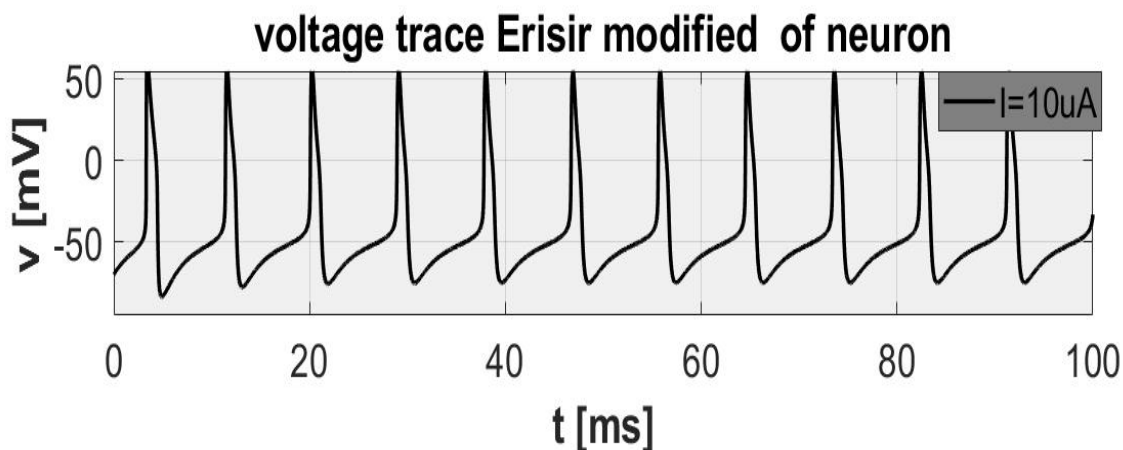


Figure 3.15 Voltage trace of modified Erisir neuron with potassium conductance equal to g_{Kn4} instead of g_{Kn2} , $I = 10 \mu A/cm^2$ [7]. In Figures 3.13, 3.14, and 3.15 above, it shows the voltage trace with $I = 7, 6, \text{ and } 10 \mu A/cm^2$ respectively. These figures represent voltage independent time, and each time a different injection current or a stimulate current. This means that by increasing a current, the frequency increases with constant voltage and time values. If the current value is higher than the threshold value for generation the action potential.



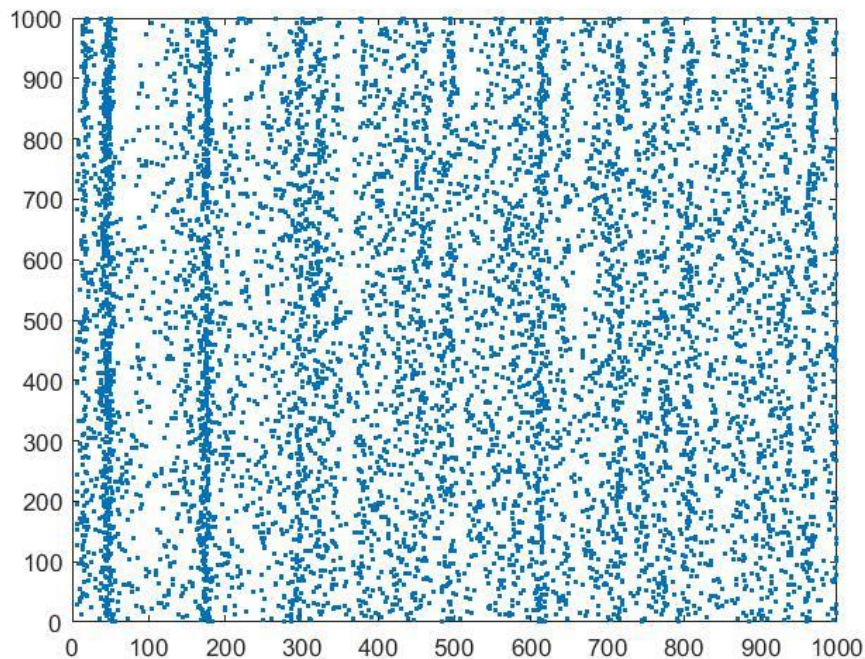


Figure 3.16 Simulation of a network of 1000 randomly coupled spiking neurons [9]

Top: spike raster shows episodes of alpha and gamma band rhythms (vertical lines). Bottom: typical spiking activity of an excitatory neuron. All spikes are equalize at +30 mV by resetting v first to +30 mV and then to c .

Izhikevich Model exhibits all neuron behaviors. In addition it is widely used in benchmarking and simulation of spiking neural networks. that the network exhibits asynchronous cortex-like dynamics; That is, the neurons release the medium Poisson spike Shooting rates are around 8 Hz. Dark vertical lines refer to the presence of transverse loops of simultaneous launches in the alpha and gamma frequency range (10 and 40 Hz, respectively). Types of group behavior, including spindle waves and sleep oscillation. We can easily notice and study these cortical states because we have. The simple ripple model accurately demonstrates the dynamics of known species of cortical neurons. Thus, there is no longer a contradiction between. Biological plausibility and computational efficiency of the nervous model network.

Discussion and Conclusions

The five various mentioned neuron models are described and demonstrated. This section provides a comparison between them in terms of computational efficiency, number of variables. In addition, the five neuron models are compared in terms of their biological plausibility. Hodgkin-Huxely model exhibit all neural behaviors which will be used in applications where every single detail is needed, but this model require very huge computational power. Izhikevich model exhibit most of neural behaviors and does not require huge computational power, which it is the best model that can used in any simulation or implementation of spiking neural networks, e.g. hippocampus simulation, classification, or solving engineering problems.

Future Work

The spiking neuron models can be used.to help us in designing invasive artificial hand. As we will have a broader field and understanding of the nervous signals and thus control the artificial hand or the artificial eye, it is also possible make systems similar to the work of the nervous system.

Appendix A

The Hodgkin Huxley Code

clc

clear all

%%%%%%%%%%5 this code is base code

global C v_na v_k g_na g_k v_l g_l I

C=1E0;

v_na=45;

v_k=-82;

g_na=120;

g_k=36;

v_l=-59;

g_l=0.3;

I=10E0;

v0=-50;

h0=.6;

m0=0.4;

n0=0.4

tend=50;

dt=0.01;

y0=[v0 m0 h0 n0];

%[t,y]=ode45(@set_ode,[0 tend],y0);

i=1;

for tt=dt:dt:tend

 y(i,1:4)=y0;

 t(i)=tt;

 dy=set_ode(tt,y0);

 y0=y0+dt*dy';

 i=i+1;

end

figure(1)

plot(t,y(:,1),'r','LineWidth',2)

xlabel('time (s)','FontName','TimeNewsRoman','FontWeight','Bold','Color','b');

ylabel('v','FontName','TimeNewsRoman','FontWeight','Bold','Color','b')

figure(2)

plot(t,y(:,2),'b','LineWidth',2)

hold on

plot(t,y(:,3),'g','LineWidth',2)

plot(t,y(:,4),'r','LineWidth',2)

xlabel('time (s)','FontName','TimeNewsRoman','FontWeight','Bold','Color','b');

ylabel('v','FontName','TimeNewsRoman','FontWeight','Bold','Color','b')

legend('m','h','n')

```
function dy = set_ode( t,y )
%%%%%%%%%%
%UNTITLED2 Summary of this function goes here
% Detailed explanation goes here

global C v_na v_k g_na g_k v_l g_l I

v=y(1);

alfa(2)=(v+45)./10/(1-exp(-(v+45)/10));
beta(2)=4*exp(-(v+70)/18);

alfa(3)=0.07*exp(-(v+70)/20);
beta(3)=1/(1+exp(-(v+40)/10));

alfa(4)=0.01*(v+60)/(1-exp(-(v+60)/10));
beta(4)=exp(-(v+70)/80)/8;

dy(1,1)=(g_na*y(2)^3*y(3)*(v_na-y(1))+g_k*y(4)^4*(v_k-y(1))...
    +g_l*(v_l-y(1))+I)/C;

for i=2:4
dy(i,1)=alfa(i)*(1-y(i))-y(i)*beta(i);
end

end
```

Appendix B

The Izhikevich Code

```
Ne=800; Ni=200;
re=rand(Ne,1); ri=rand(Ni,1);
a=[0.02*ones(Ne,1); 0.02+0.08*ri];
b=[0.2*ones(Ne,1); 0.25-0.05*ri];
c=[-65+15*re.^2; -65*ones(Ni,1)];
d=[8-6*re.^2; 2*ones(Ni,1)];
S=[0.5*rand(Ne+Ni,Ne), -rand(Ne+Ni,Ni)];
v=-65*ones(Ne+Ni,1); % Initial values of v
u=b.*v; % Initial values of u
firings=[]; % spike timings
for t=1:1000 % simulation of 1000 ms
I=[5*randn(Ne,1);2*randn(Ni,1)]; % thalamic input
fired=find(v>=30); % indices of spikes
firings=[firings; t+0*fired,fired];
v(fired)=c(fired);
u(fired)=u(fired)+d(fired);
I=I+sum(S(:,fired),2);
v=v+0.5*(0.04*v.^2+5*v+140-u+I); % step 0.5 ms
v=v+0.5*(0.04*v.^2+5*v+140-u+I); % for numerical
u=u+a.*(b.*v-u); % stability
end;
plot(firings(:,1),firings(:,2),'.');
```

References

1. Borisyuk, Alla, et al. *Tutorials in mathematical biosciences I: mathematical neuroscience*. Springer, 2005.
2. Rhoda, Kristen M., Mary Jo Porter, and Cristiano Quintini. "Fluid and electrolyte management: putting a plan in motion." *Journal of Parenteral and Enteral Nutrition* 35.6 (2011): 675-685.
3. Mason, Emily R. *Epilepsy Mutations in Different Regions of the Nav1. 2 Channel Cause Distinct Biophysical Effects*. Diss. 2020.
4. Corkins, Mark R., ed. *The ASPEN pediatric nutrition support core curriculum*. American Society for Parenteral and Enteral Nutrition, 2015.
5. [5] Meyers, Rachel S. "Pediatric fluid and electrolyte therapy." *The Journal of Pediatric Pharmacology and Therapeutics* 14.4 (2009): 204-211.
6. [6] RD, KEYNES, and LEWIS PR. "The sodium and potassium content of cephalopod nerve fibers." *The Journal of Physiology* 114.1-2 (1951): 151-182.
7. [7] Börgers, Christoph. *An introduction to modeling neuronal dynamics*. Vol. 66. Cham: Springer, 2017.
8. [8] Dayan, Peter, and Laurence F. Abbott. "Theoretical neuroscience: computational and mathematical modeling of neural systems." *Journal of Cognitive Neuroscience* 15.1 (2003): 154-155.
9. [9] Wallisch, Pascal, et al. *MATLAB for neuroscientists: an introduction to scientific computing in MATLAB*. Academic Press, 2014.
10. [10] Lindsay, K. A., et al. "An introduction to the principles of neuronal modelling." *Modern techniques in neuroscience research*. Springer, Berlin, Heidelberg, 1999. 213-306.
11. [11] Abu Snaina, Ahmed, and Rosni Abdullah. "Spiking neuron models: a review." (2014).
12. [12] Hodgkin, Alan L., and Andrew F. Huxley. "A quantitative description of membrane current and its application to conduction and excitation in nerve." *The Journal of physiology* 117.4 (1952): 500.
13. [13] Siciliano, Ryan. "The Hodgkin–Huxley model—its extensions, analysis and numerics." McGill Univ., Dept. Math. and Statist., Montreal, Canada (2012).
14. [14] Izhikevich, Eugene M. "Simple model of spiking neurons." *IEEE Transactions on neural networks* 14.6 (2003): 1569-1572.